

# APPLICATION OF THE REDUCTION OF SCALE RANGE IN A LORENTZ BOOSTED FRAME TO THE NUMERICAL SIMULATION OF PARTICLE ACCELERATION DEVICES \*

J.-L. Vay<sup>†</sup>, W. M. Fawley, C. G. R. Geddes, E. Cormier-Michel, LBNL, Berkeley, CA, USA  
D. P. Grote, LLNL, Livermore, CA, USA

## Abstract

It has been shown [1] that it may be computationally advantageous to perform computer simulations in a boosted frame for a certain class of systems: particle beams interacting with electron clouds, free electron lasers, and laser-plasma accelerators. However, even if the computer model relies on a covariant set of equations, it was also pointed out that algorithmic difficulties related to discretization errors may have to be overcome in order to take full advantage of the potential speedup [2]. In this paper, we focus on the analysis of the complication of data input and output in a Lorentz boosted frame simulation, and describe the procedures that were implemented in the simulation code Warp[3]. We present our most recent progress in the modeling of laser wakefield acceleration in a boosted frame, and describe briefly the potential benefits of calculating in a boosted frame for the modeling of coherent synchrotron radiation.

## INTRODUCTION

In [1], we have shown that the ratio of longest to shortest space and time scales of a system of two or more components crossing at relativistic velocities is not invariant under a Lorentz transformation. This implies the existence of a frame of reference minimizing an aggregate measure of the ratio of space and time scales. It was demonstrated that this translated into a reduction by orders of magnitude in computer simulation run times, using methods based on first-principles (e.g., Particle-In-Cell), for particle acceleration devices or problems such as: particle beams interacting with electron clouds, free electron lasers, and laser-plasma accelerators. In [2], we have shown that in order to take the full benefits of the calculation in a boosted frame, some of the standard numerical techniques needed to be revised, and proposed a new particle pusher which improves upon the standard Boris pusher [4] for the handling of relativistic particles. An additional practical complication that is introduced by simulating in a boosted frame is that inputs and outputs are often known, or desired, in the labo-

ratory frame. We explain in this paper how we handle this later complication into the accelerator PIC code Warp [3], present our latest results on the modeling of laser plasma wakefield acceleration in a boosted frame, and briefly describe the potential benefits of calculating in a boosted frame for the modeling of coherent synchrotron radiation.

## INPUT AND OUTPUT OF DATA TO AND FROM A BOOSTED FRAME SIMULATION

So far, it has been common practice to perform simulations in the laboratory frame, for direct comparison with experimental results, or in another frame (beam frame, center of mass frame, etc.) which offers an advantage of symmetry, simplification, or other convenience, in comparing the results to those of analytical theory or experiment. However, the analysis that was provided in [1] shows that the frame that will minimize the computational requirements may not be any of the above. In this case, one may need to apply Lorentz transformations between the frame of calculation and the frame in which input data are known and/or the frame in which the output data are desired. Because of the relativity of simultaneity that is inherent to the Lorentz transformation, this requires a process that goes beyond a mere algebraic manipulation of data. In the implementation of such process in the code Warp, we have found convenient to input data (particles or fields) through a plane, as well as to output data at series of planes, all of which are perpendicular to the direction of the relative velocity between the frame of calculation and the other frame of choice. For illustration purposes, we take as an example in this paper the test case that was presented in [1] of an ion beam interacting with a background of electrons, in an assumed continuous transverse focusing system, leading to a growing transverse instability. We present in this section in more detail the techniques that were used to input and output the data. We note that the careful implementation of these techniques was essential for the very high level of agreement that was obtained in [1] between a calculation in the laboratory frame and a calculation in a boosted frame.

### Input

**Particles:** In the laboratory frame, the electron background is initially at rest and a moving window is used to follow the beam progression. Traditionally, the beam macroparticles are initialized all at once in the window, while background electron macroparticles are created con-

\* This work was supported under the auspices of the U.S. DOE by Univ. of Calif., LBNL and LLNL under contracts DE-AC02-05CH11231 and DE-AC52-07NA27344, the U.S.-LHC Accelerator Research Program (LARP), and the U.S. Department of Energy, Office of Science grant of the SciDAC program, Community Petascale Project for Accelerator Science and Technology (ComPASS). This research used resources of the National Energy Research Scientific Computing Center, which is supported by the Office of Science of the U.S. Department of Energy under Contract No. DE-AC02-05CH11231.

<sup>†</sup> jlvay@lbl.gov

tinuously in front of the beam on a plane that is perpendicular to the beam velocity. In a frame moving at some fraction of the beam velocity in the laboratory frame, the beam initial conditions at a given time are generally unknown and one must initialize the beam differently. Given the position and velocity  $\{x, y, z, v_x, v_y, v_z\}$  for each beam macroparticle at time  $t = 0$ , we follow the following procedure for transforming the beam quantities for injection in a boosted frame moving at  $\beta_f c$  in the laboratory:

1. project positions at  $z^* = 0$

$$t^* = (z - \bar{z}) / v_z \quad (1)$$

$$x^* = x - v_x t^* \quad (2)$$

$$y^* = y - v_y t^* \quad (3)$$

$$z^* = 0 \quad (4)$$

(the velocity components are left unchanged)

2. apply Lorentz transformation from laboratory frame to boosted frame

$$t'^* = -\gamma_f t^* \quad (5)$$

$$x'^* = x^* \quad (6)$$

$$y'^* = y^* \quad (7)$$

$$z'^* = \gamma_f \beta_f c t^* \quad (8)$$

$$v_x'^* = \frac{v_x^*}{\gamma_f (1 - \beta_f \beta)} \quad (9)$$

$$v_y'^* = \frac{v_y^*}{\gamma_f (1 - \beta_f \beta)} \quad (10)$$

$$v_z'^* = \frac{v_z^* - \beta_f c}{1 - \beta_f \beta} \quad (11)$$

(where  $\gamma_f = 1/\sqrt{1 - \beta_f^2}$ )

3. synchronize macroparticles in boosted frame

$$z' = z'^* - \bar{v}_z'^* t'^* \quad (12)$$

(the transverse position and the velocity components are left unchanged, "frozen" until the macroparticle passes through the injection plane).

In this procedure, we take advantage of the fact that the beam initial conditions are often known for a given plane in the laboratory, either directly or via simple calculation or projection from the conditions at a given time (step 1). From these, the initial conditions of the beam at the same plane in a boosted frame are trivially known via a Lorentz transformation (step 2). With the knowledge of the time at which each beam macroparticle crosses the plane into consideration, one can inject each beam macroparticle in the simulation at the appropriate location and time.

The procedure for injecting the macroparticles is not sufficient for setting the electrostatic or electromagnetic fields at the plane of injection. By default, our code computes the three-dimensional fields from solving the Poisson or the

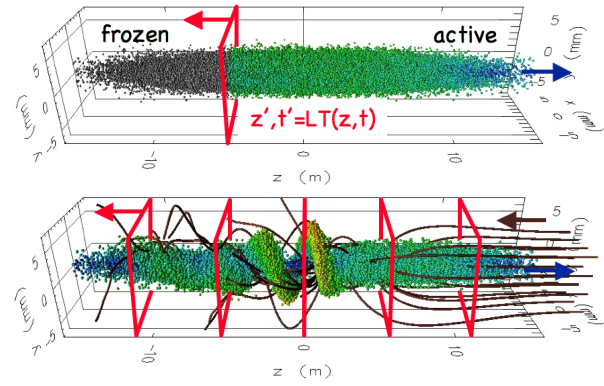


Figure 1: (top) Snapshot of the beam "frozen" (grey spheres) and "active" (colored spheres) macroparticles traversing the injection plane (red rectangle). (bottom) Snapshot of the beam macroparticles (colored spheres) passing through the background of electrons (dark brown streamlines) and the diagnostic stations (red rectangles). The electrons, the injection plane and the diagnostic stations are fixed in the laboratory plane, and are thus counterpropagating to the beam in a boosted frame.

Maxwell equations on a grid on which the source term, respectively charge or current density, is obtained from the macroparticles distribution. This requires generation of a three-dimensional representation of the beam distribution of macroparticles at a given time before they cross the injection plane. This is accomplished (step 3) by expanding the beam distribution longitudinally such that all macroparticles are synchronized to the same time in the boosted (so far known at different time of arrival at the injection plane), and setting the beam distribution as "frozen" macroparticles which undergo a special treatment: the three velocity components and the two position components perpendicular to the boosted frame velocity are fixed, while the remaining position component is advanced at the average beam velocity. Figure 1 (top) shows a snapshot of a beam that has passed partly through the injection plane. As the frozen beam macroparticles pass through the injection plane (which move opposite to the beam in the boosted frame), they are converted to "active" macroparticles. The charge or current density is accumulated from the active and the frozen particles, thus ensuring that the fields at the plane of injection are consistent.

**Laser:** The laser is generally injected through a plane, using a three-dimensional analytical formula, which is straightforward to transform into a boosted frame using the Lorentz transformation of electromagnetic fields. The only minor complication is that the plane is moving at a constant velocity in the boosted frame, which is readily handled by interpolating the data from the injection plane onto the mesh used for electromagnetic calculations.

## Output

For the output, we have found it convenient to record quantities at a number of regularly spaced “stations”, immobile in the laboratory frame, at a succession of discrete times to record data history or averaged over time. Since the space-time locations of the diagnostic grids in the laboratory frame generally do not coincide with the space-time positions of the macroparticles and grid nodes used for the calculation in a boosted frame, some interpolation is performed during the data gathering process. A visual example is given on Fig. 1 (bottom).

## EXAMPLES OF APPLICATION

In [1], we showed that simulations in a boosted frame may benefit the study of (a) the interaction of relativistic beams with electron clouds in particle accelerators, (b) free electron lasers and (c) laser wakefield acceleration. Examples of (a) were given in [1] and [2], while examples of (b) are available in [5] and [6], where it was concluded that “if the necessary FEL physics can be studied with an eikonal code, it will be much faster than a full EMcode (in whatever frame). However, if there are optical or shorter wavelength physics that cannot be resolved properly by an eikonal code with its underlying slowly-varying envelope approximation, a boosted-frame EM code is a very attractive option”.

We concentrate in this paper on recent simulations in boosted frames of (c) with the code Warp. Other examples of (c) in boosted frames from two other research groups are given in [7], [8] and [9].

### Warp Calculation of a Scaled Stage of a Laser Wakefield Accelerator

Laser driven plasma waves offer orders of magnitude increases in accelerating gradient over standard accelerating structures (which are limited by electrical breakdown), thus holding the promise of much shorter particle accelerators. Yet, computer modeling of the wake formation and beam acceleration requires fully kinetic methods and large computational resources due to the wide range of space and time scales involved [10]. For example, modeling 10 GeV stages for the LOASIS BELLA proposal [11] in one-dimension demanded as many as 5,000 processor hours on a NERSC supercomputer [7]. As discussed in [1], the range of scales can be greatly reduced if one adopts the common assumption that the backward emitted radiation can be neglected.

We have performed with Warp a series of four 2-1/2D simulations in frames moving respectively at  $\gamma_f = 1$  (laboratory frame), 2, 5, and 10, using the set of parameters given in table 1, corresponding to a case with  $k_p L = 2$ . Simulations, at  $n_e = 10^{19} \text{ cm}^{-3}$ , are scaled replicas of 10 GeV stages that would operate at  $10^{17} \text{ cm}^{-3}$  [12]. The high density results in short run time for effective benchmarking between the algorithms.

### Beam Dynamics and Electromagnetic Fields

#### D05 - Code Developments and Simulation Techniques

Table 1: List of parameters for the LWFA simulations.

beam radius	$R_b$	82.5 nm
beam length	$L_b$	82.5 nm
beam peak density	$n_b$	$10^{20} \text{ m}^{-3}$
laser longitudinal profile		sinusoidal
laser transverse profile		gaussian
laser length (FWHM)	$L$	$3.36 \mu\text{m}$
laser size	$\sigma$	$8.91 \mu\text{m}$
laser wavelength	$\lambda$	$0.8 \mu\text{m}$
normalized vector potential	$a_0$	1
plasma density	$n_p$	$10^{19} \text{ cm}^{-3}$
plasma ramp profile		half sinus
plasma ramp length		$4 \mu\text{m}$

Figure 2 shows surface renderings of the longitudinal electric field as the beam is in its early stage of acceleration by the plasma wake from the calculation in the laboratory frame and in the frame  $\gamma_f = 10$ . The two snapshots offer strikingly different views of the same physical processes: in the laboratory frame, the wake is fully formed before the beam undergoes any significant acceleration and the imprint of the laser is clearly visible, while in the boosted frame calculation, the beam is accelerated as the plasma wake develops, and the laser imprint is not visible on the snapshot. Without additional diagnostics, it is impossible to assert the degree of agreement between the two simulations.

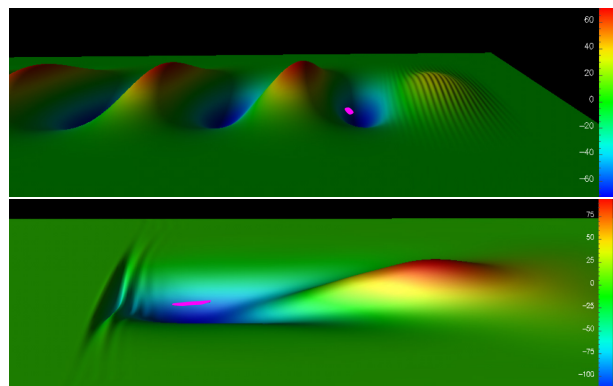


Figure 2: Colored surface rendering of the longitudinal electric field from a 2-1/2D Warp simulation of a laser wakefield acceleration stage in the laboratory frame (top) and a boosted frame at  $\gamma_f = 10$  (bottom), with the beam (magenta) in its early phase of acceleration.

Histories of the perpendicular and longitudinal electric field recorded at a number of stations at fixed locations in the laboratory allow direct comparison between the simulations in different reference frames. Figure 3 shows such a diagnostic for the four abovementioned runs at the positions (in the laboratory frame)  $z_1 = 0.154 \text{ mm}$  and  $z_2 = 1.354 \text{ mm}$  and for  $x = y = 0$ . The agreement

is excellent at station  $z_1$ , located near the entrance of the plasma, but is not as good at station  $z_2$  located further downstream, where two groups emerge, with agreement between runs at  $\gamma_f = 1$  and  $\gamma_f = 2$ , and between  $\gamma_f = 5$  and  $\gamma_f = 10$ .

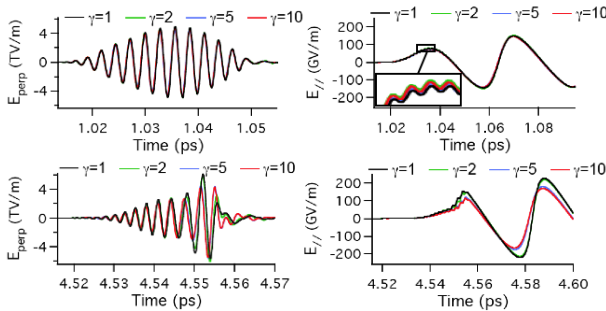


Figure 3: History of perpendicular (left) and longitudinal (right) electric field at the positions (in the laboratory frame)  $x = y = 0$ ,  $z_1 = 0.154\text{mm}$  (top) and  $z_2 = 1.354\text{mm}$  (bottom) from simulations in the laboratory frame (black) and boosted frames at  $\gamma_f = 2$  (green), 5 (blue), and 10 (red).

The average beam energy as a function of position in the laboratory frame is plotted in Figure 4 and very good agreement is obtained, with again a separation in the same two groups as with the electric field diagnostics. The CPU time recorded as the beam crosses successive stations in the laboratory frame is plotted in Figure 5. The total CPU time for the run in the laboratory frame was about 2500 seconds while it was around 25 seconds for the run in the frame at  $\gamma_f = 10$ , demonstrating a 100 times speedup for the later. The gain in efficiency scales roughly as  $1/n$  where  $n$  is the plasma density. Studies are hence in progress to use boosted frame simulations to directly simulate 10 GeV stages at plasma densities of  $10^{17}\text{ cm}^{-3}$ , which are not presently computationally accessible using conventional explicit simulations.

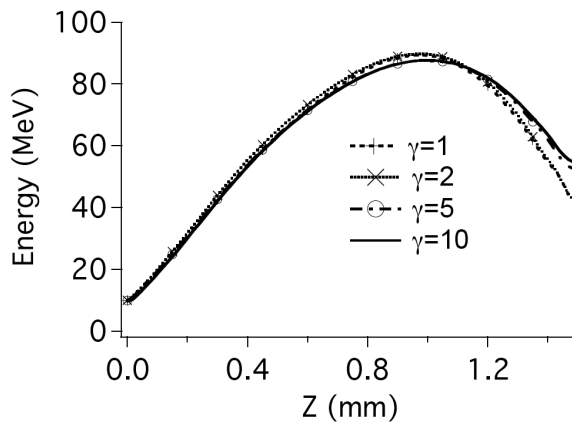


Figure 4: Average beam energy versus longitudinal position in the laboratory frame from calculations in a frame moving at  $\gamma_f = 1, 2, 5$  and 10.

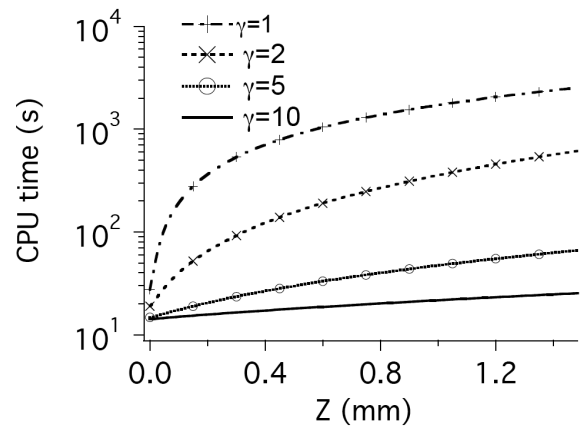


Figure 5: CPU time recorded as the beam crosses successive stations in the laboratory frame.

### Modeling of Coherent Synchrotron Radiation in a Boosted Frame

Another application for which the Lorentz-boosted frame method might be useful is that of modeling coherent synchrotron radiation (CSR) emitted by high current, high brightness relativistic electron beams. Many applications of such beams (e.g., short wavelength free-electron lasers) rely upon longitudinal beam compression in dispersive chicanes consisting of dipole magnets. High current electrons beams in such chicanes can emit copious CSR which leads both to energy variations along the electron beam and growth in the beam's projected transverse emittance. Because full scale EM simulation of CSR in the lab frame is difficult due to the wide range of scales (chicane lengths of order meters, radiation wavelengths of orders microns), most simulation codes modeling CSR effects apply simplifications such as ignoring transverse variation of CSR across the e-beam in order to make the calculation tractable.

We have begun preliminary work of simulating CSR emission with the boosted frame method examining the behavior of a high current, short e-beam transiting a simple dipole magnet. We have picked a Lorentz frame whose transformation velocity  $v_z = v_0 \cos(\phi/2)$  where  $\phi$  is the dipole's bend angle and  $v_0$  is the initial electron beam velocity. Our early results show that upon exit from the undulator the electron beam shows the characteristic energy variation with longitudinal position that one expects from previous theoretical analyses of CSR. However, there remains much work to be done concerning determination of the necessary grid and time resolution and further optimizing the calculation for higher speed, e.g., via application of appropriate moving windows and mesh refinement methods.

## CONCLUSION

In this paper, we focused on the analysis of the complication of data input and output in a Lorentz boosted frame simulation, and described the procedure that were implemented in the simulation code Warp. We also showed good agreement between 2-1/2D Warp simulations of one acceleration stage of laser plasma acceleration in the laboratory frame and in three boosted frames, with gamma of 2, 5 and 10 for a maximum measured speedup of 100. The remaining discrepancies are under investigation. Similar simulations are planned in three dimensions, and for higher beam density, where beam loading becomes significant. Other examples of simulations of LWFA in boosted frames from two other research groups are described in [7], [8] and [9].

Finally, we identified another possible application. Coherent synchrotron emission from high current, high brightness relativistic electron beams involves a wide range of space and time scales, and most simulation codes modeling CSR effects apply simplifications such as ignoring transverse variation of CSR across the e-beam in order to make the calculation tractable. Simulating in a boosted frame may render possible full three-dimensional modeling of coherent synchrotron radiation, which is ultimately needed for an accurate description of the process.

The recent progress show that modeling in a Lorentz boosted from first principle is a viable alternative or complement to using reduced descriptions like the quasistatic or eikonal approximations, or scaled parameters as in [12], for example, when there is a need to study physics that is not accessible to the other descriptions, or for their validation.

We are thankful to D. L. Bruhwiler, J. R. Cary, E. Esarey, S. F. Martins, W. B. Mori, B. A. Shadwick and C. B. Schroeder for insightful discussions.

## REFERENCES

- [1] J.-L. Vay, 'Noninvariance of space- and time- scale ranges under a Lorentz transformation and the implications for the study of relativistic interactions', Phys. Rev. Lett., 98 (2007) 130405.
- [2] J.-L. Vay, 'Noninvariance of space- and time- scale ranges under a Lorentz transformation and the implications for the study of relativistic interactions', Phys. Plas., 15 (2008) 056701.
- [3] D. P. Grote, A. Friedman, J.-L. Vay, I. Haber, AIP Conf. Proc. 749 (2005) 55.
- [4] J. P. Boris, 'Relativistic plasma simulation-optimization of a hybrid code', Proc. Fourth Conf. Num. Sim. Plasmas, Naval Res. Lab., Wash., D. C., 3-67, 2-3 November 1970.
- [5] W. M. Fawley, J.-L. Vay, 'Use of the Lorentz-boosted frame transformation to simulate free-electron laser amplifier physics', Proceedings of the 13th Advanced Accelerator Concepts Workshop, Santa Cruz, CA (2008) 346.
- [6] W. M. Fawley, J.-L. Vay, 'Full electromagnetic simulation of free-electron laser amplifier physics via the Lorentz-boosted frame approach', These proceedings, WE5RFP029

- [7] D. L. Bruhwiler et al, 'New developments in the simulation of advanced accelerator concepts', Proceedings of the 13th Advanced Accelerator Concepts Workshop, Santa Cruz, CA (2008) 29.
- [8] S. F. Martins et al, 'Numerical simulations of LWFA for the next generation of laser systems', Proceedings of the 13th Advanced Accelerator Concepts Workshop, Santa Cruz, CA (2008) 285.
- [9] S. F. Martins, 'Boosted frame PIC simulations of LWFA: toward the energy frontier', These proceedings, TH4GBC05
- [10] C.G.R. Geddes et al, 'Computational studies and optimization of wakefield accelerators', J. Phys. Conf. Series V 125 pp. 12002/1-11 (2008).
- [11] <http://loasis.lbl.gov>
- [12] C. G. R. Geddes et al, "Multi-GeV Laser Wakefield Accelerator Stages and Controlled Injection", These proceedings WE6RFP075